whose determinant is equal to 4 and is therefore convex. f_g is stated as a quadratic polynomial of one variable with a leading positive coefficient and therefore is also convex. Because f_g is convex and h_g is convex then the generator cost terms together form a convex function. The demand-bus revenue terms take the form $\sum_d f_d(h_d(V_{Rd}, V_{Id}))$. h_d is an affine map. f_d is a sum of two quadratic polynomials of one variable with a leading positive coefficient and therefore is convex. The composition of a convex function with an affine map is also convex. Eqs. 69-73 are all stated in terms of two (separable) variables and have Hessians whose determinant is equal to 4. The remaining constraints are all linear and create a convex polyhedral feasible region. Therefore, they are convex as well. Because all the constraints are convex and the objective function is convex, the optimization program is also convex. □

IV. NEWTON-RAPHSON (NR) SOLUTION ALGORITHM FOR THE IV-ACOPF FORMULATION

This section presents a Newton-Raphson Solution Algorithm for the *unrelaxed* IV-ACOPF formulation to *global optimality in polynomial time*. First, Theorem 1 provides a solid foundation upon which to solve the *relaxed* IV-ACOPF via Newton-Raphson gradient descent to a candidate solution $y^\dagger$. If $y^\dagger$ is found within the (unrelaxed) feasible $\mathcal{R}_F$, then the algorithm has found a global solution. If $y^\dagger$ is found within the relaxed region $\mathcal{R}_R$, then it must be discarded as infeasible because the $\mathcal{R}_F$ (as we prove below) is infeasible.

To begin, because the *relaxed* IV-ACOPF is a convex optimization program and fulfills Slater's Condition [100], it may be solved straightforwardly by formulating the Lagrangian, deriving the first order optimality (KKT - Karush-Kuhn-Tucker) conditions, and solving using a Newton-Raphson algorithm. The standard form of a convex optimization program is:

$$\text{Minimize} \quad \mathcal{J}(x) \tag{79}$$

$$\text{s.t} \quad h(x) = 0 \tag{80}$$

$$g(x) \leq 0 \tag{81}$$

where $\mathcal{J}(x)$ and $g(x)$ are convex functions and $h(x)$ is an affine function. In this work, $x = [V_{RG}; V_{IG}; I_{RG}; I_{IG}; V_{RD}; V_{ID}]$. Furthermore, h(x) is represented by Equations 60 - 64 and g(x) is represented by Equations 65 - 76. The Lagrangian is:

$$\mathcal{L}(y) = f(x) + \lambda^T h(x) + \mu^T g(x) \tag{82}$$

where $y = [x; \lambda; \mu]$. The first order (KKT) optimality conditions follow straightforwardly from $\nabla\mathcal{L}$.

$$\nabla f(x) + \mu^T \nabla g(x) + \lambda^T \nabla h(x) = 0 \tag{83}$$

$$h(x) = 0 \tag{84}$$

$$g(x) \leq 0 \tag{85}$$

$$\mu \geq 0 \tag{86}$$

$$\mu^T g(x) = 0 \tag{87}$$

where Eq. 83 is the stationarity condition, Eq. 84 and 85 assure primal feasibility, Eq. 86 assures dual feasibility, and Eq. 87 assures complementary slackness. Finally, the Newton-Raphson Algorithm 1 is applied with H_k as the k^{th} iterate of the Hessian of the Lagrangian.

Algorithm 1 Newton-Raphson Minimization Algorithm for Unrelaxed IV-ACOPF Formulation

```
procedure ACOPF(k = 0, y_0, ε)
    while ||∇L(y_i)|| < ε do
        y_{k+1} ← y_k + H_k^{-1} ∇L(y_k)
        k ← k + 1
    end while
    y† ← y_k
    if y† ∈ R_F then
        y* ← y†
    else
        y* ← Ø
    end if
    return y*
end procedure
```

Theorem 2: Algorithm 1 converges quadratically to a globally optimal solution to the *unrelaxed* IV-ACOPF formulation (defined by Eqs 59-72 and 77) in polynomial-time.

Proof: At a high level, Algorithm 1 is composed of two subsections. In the first, the While Loop implements the well-known Newton-Raphson algorithm to produce the candidate solution $y^\dagger$. The algorithm has a quadratic convergence rate [100] and gives a globally optimal solution to convex optimization problems in polynomial time [110]–[112]. In the second subsection, a test is made on the candidate solution. If $y^\dagger \in \mathcal{R}_F$, then the Newton-Raphson algorithm has found the global optimum. In all other cases, $y^\dagger \in \mathcal{R}_\mathcal{R}$ then by Lemma 1 (below), $\mathcal{R}_F = \emptyset$ and the candidate solution $y^\dagger$ must be discarded and an infeasible solution returned instead. Therefore, Algorithm 1 either finds the globally optimal solution or infeasible solution in polynomial time. □

Lemma 1: If Algorithm 1 returns a candidate solution $y^\dagger \in \mathcal{R}_R$, then $\mathcal{R}_F = \emptyset$.

Proof: A proof by contradiction is is provided. Assume that $\mathcal{R}_F \neq \emptyset$.

1) First recognize that Algorithm 1 *always* returns $|V_G^\dagger| = \overline{|V_G|}$. Because the objective function must minimize generator currents $\mathcal{I}_G$ without consideration for generator terminal voltages, the generator terminal voltages, by Ohm's Law, must rise to their maximal value.
2) In the meantime, an increase of demand-bus voltage magnitudes from $|V_D^\dagger|$ to a hypothetical value $|V_D^\ddagger| = |V_D^\dagger + \Delta V_D|$ where $|\Delta V_D| > 0$ so that $\underline{|V_D|} \leq |V_D^\ddagger| \leq \overline{|V_D|}$, by Lemma 2 (below), *necessitates* an increase in one or more generator voltage magnitudes from $|V_G^\dagger|$ to $|V_G^\ddagger| = |V_G^\dagger + \Delta V_G|$. Because $|V_G^\dagger| = \overline{|V_G|}$, $|V_G^\ddagger| > \overline{|V_G|}$ creates a contradiction where the generator terminal voltage upper bound is violated.

Therefore, by contradiction, if $y^\dagger \in \mathcal{R}_R$, then $\mathcal{R}_F = \emptyset$. □

The importance of Lemma 1 to Theorem 2 (as the main result of the paper) cannot be understated. Because this paper uses a steady-state current injection model, it has generator terminal voltages. These generator terminal voltages, in turn, have upper bounds. Any effort to move the demand-bus voltage magnitudes upwards will require the generator terminal voltage magnitudes to move upward as well, and beyond their upper bound values. Therefore, if the demand-bus voltage magnitudes are lower than the lower bounds, then there is no way to increase them without violating the generator terminal voltage upper bounds instead. The reader will recognize that the argument of the Lemma 1 proof presented above is built upon a physical intuition rooted in Ohm's Law: an increase in one of more demand-bus voltage magnitudes necessitates an increase in one or more generator terminal voltage magnitudes. Practicing electrical engineers will recognize this physical intuition as always true by experience. Nevertheless, for a purely mathematical argument, this statement is recast as Lemma 2 below.

Lemma 2: An increase of demand-bus voltage magnitudes from $|V_D^\dagger|$ to a hypothetical value $|V_D^\ddagger| = |V_D^\dagger + \Delta V_D|$ where $|\Delta V_D| > 0$ *necessitates* an increase in one or more generator voltage magnitudes from $|V_G^\dagger|$ to $|V_G^\ddagger| = |V_G^\dagger + \Delta V_G|$.

Proof: A proof by contradiction is provided. First, for simplicity, Equations 10, 11, 18 and 19 are combined into a single linear matrix equality over complex numbers

$$\begin{bmatrix} \mathcal{I}_G^\dagger \\ -\mathcal{I}_D \end{bmatrix} = Y \begin{bmatrix} V_G^\dagger \\ V_D^\dagger \end{bmatrix} = \begin{bmatrix} Y_{GG} & Y_{GD} \\ Y_{DG} & Y_{DD} \end{bmatrix} \begin{bmatrix} V_G^\dagger \\ V_D^\dagger \end{bmatrix} \tag{88}$$

where the bus admittance matrix $Y = G + jB$ is partitioned into $Y_{GG} = [A_G^T Y_L A_G]$, $Y_{GD} = [A_G^T Y_L A_D]$, $Y_{DG} = [A_D^T Y_L A_G]$, and $Y_{DD} = [A_D^T Y_L A_D]$. Taking the gradient of both sides yields:

$$\begin{bmatrix} \Delta \mathcal{I}_G \\ 0 \end{bmatrix} = \begin{bmatrix} Y_{GG} & Y_{GD} \\ Y_{DG} & Y_{DD} \end{bmatrix} \begin{bmatrix} \Delta V_G \\ \Delta V_D \end{bmatrix} \tag{89}$$

If we assume $\Delta V_G = 0$, then $0 = Y_{DD} \Delta V_D$. Because Y_{DD} is invertible, the only solution to this equation is $\Delta V_D = 0$. $|\Delta V_D| > 0$ is impossible. Therefore, by contradiction, a demand bus voltage increment $|\Delta V_D| > 0$ necessitates a generator terminal voltage increment *magnitude* $|\Delta V_G| > 0$. Finally, a "real-life" electric power system has power lines with positive resistances and reactances. Therefore, $G(i,j) > 0 \ \forall i = j$, $G(i,j) \leq 0 \ \forall i \neq j$, $B(i,j) < 0 \ \forall i = j$, and $B(i,j) \geq 0 \ \forall i \neq j$. Therefore, the *direction* of the voltage magnitude increment $|\Delta V_G|$ necessitates an *increase* one or more generator voltage magnitudes from $|V_G^\dagger|$ to $|V_G^\ddagger| = |V_G^\dagger + \Delta V_G|$. □

V. NUMERICAL DEMONSTRATION

To demonstrate the profit-maximizing security-constrained IV-ACOPF, a modified version of the Saadat (1999) transient stability test case [94] is chosen. The associated one-line diagram is shown in Fig. 4. The system consists of three generator buses (in blue) and three generator lead-lines (in red), six demand buses (in green) and seven power lines (in blue). Impedance values have been retained from the original text, and the current withdrawals at the demand buses are shown on the figure. Similarly, the minimum and maximum limits on generator current injections are provided. All bus voltage magnitudes have a lower bound of 0.9 and upper bound of 1.1. The voltage stability constraint limits the angle associated with the current injected to a line between $\pm 20°$. A minimum power factor of 0.95 is used to calculate the lower limit on the demand bus voltage phase angle according to Eq. 48. The reference bus is chosen to have the largest voltage phase angle. Therefore, $\theta_{VD}^{max} = 0$. All provided values are given per unit. The chosen marginal cost ($\$/MW$) for each generator and marginal revenue values for each demand-bus are shown in Table 1.

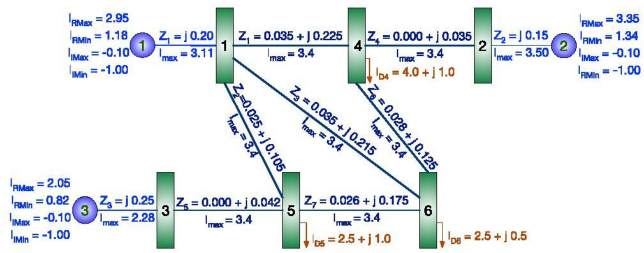

FIGURE 4. Saadat's (1999) Six Demand-Bus, Three Generator Transient Stability Test Case [94]. The topological arrangement and impedance values have been retained. Real and imaginary generator current injection are shown in green.

TABLE 1. Generator & Demand-Bus Revenue Parameters.

Generator	$\alpha_{\mathbf{Zg}}$	$\beta_{\mathbf{Zg}}$	$\gamma_{\mathbf{g}}$			
1	0.2	2	10			
2	0.1125	1.5	10			
3	0.3125	2.5	10			
Demand Bus	$\overline{\rho}_{\mathbf{Rd}}$	$\beta_{\mathbf{Rd}}$	$\overline{\gamma}_{\mathbf{Rd}}$	$\overline{\rho}_{\mathbf{Id}}$	$\beta_{\mathbf{Id}}$	$\overline{\gamma}_{\mathbf{Id}}$
1	0.25	22	130	0.025	2.2	13
2	0.30	23	130	0.030	2.3	13
3	0.26	25	130	0.026	2.5	13
4	0.28	30	130	0.028	3.0	13
5	0.20	21	130	0.020	2.1	13
6	0.29	19	130	0.029	1.9	13

These input values constitute moderate loading conditions. Here, the IV-ACOPF optimization program reaches a global optimum of $\mathcal{J} = \$763.79$. The associated decision variables are shown in Figure 5. The generators current injections remain well within their real current capacity constraints. That said, Generator 1 has reached its limit with respect to its imaginary current capacity. In the meantime, and as expected, the generator voltage magnitudes are all situated on their respective upper bounds. This is because the IV-ACOPF minimizes the cost of generator current injections but does not depend on generator voltages. Therefore, generator voltages will tend to rise in order to minimize the generator currents. At these moderate loading conditions, all

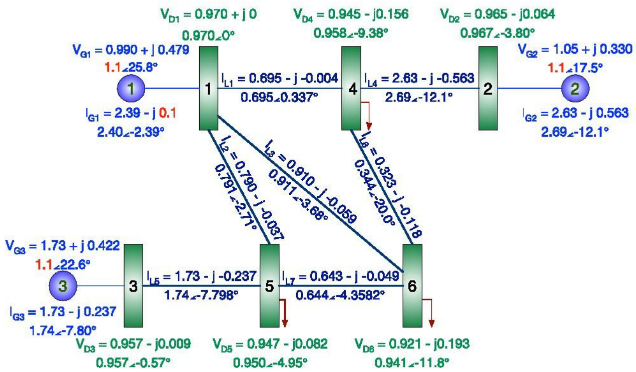

FIGURE 5. Solution of the IV-ACOPF formulation under moderate loading conditions.

of the electric power lines (including generator lead lines) remain unconstrained as well. Finally, all of the demand bus voltages are well within their voltage magnitude constraints. This rather "uneventful" scenario, nevertheless, provides an important result. Under these moderate conditions, the optimum of the relaxed IV-ACOPF is equivalent to the global optima of the unrelaxed problem. Furthermore, because there is a tendency towards higher generator terminal voltages, candidate optimal solutions $y^\dagger \in \mathcal{R}_R$ will tend to occur only when necessary, and more specifically under relatively high loading conditions. Reconsider Ohm's Law in Eq. 14. Multiplying on both sides by A_D^T and solving for V_D gives:

$$V_D = -A_1\mathcal{I}_D - A_2V_G \tag{90}$$

where

$$A_1 = (A_D^T Y_L A_D)^{-1} \tag{91}$$
$$A_2 = A_1 A_D^T Y_L A_G \tag{92}$$

In short, the network flow constraints can be rearranged so that the demand-bus voltages are written in terms of the demanded currents $\mathcal{I}_D$ and the generator terminal voltages V_G. As $\mathcal{I}_D$ increases, it pulls down demand bus voltages with it.

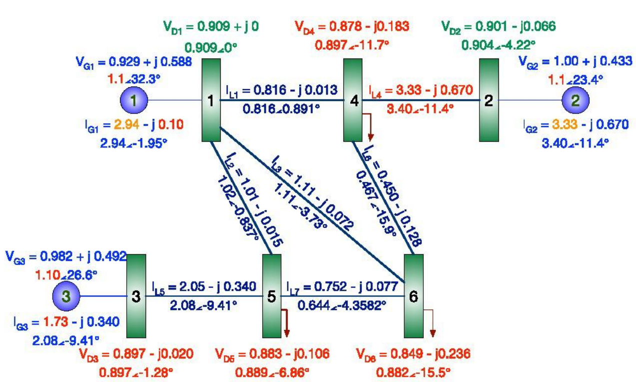

FIGURE 6. The candidate solution $y^\dagger$ of the IV-ACOPF formulation under high loading conditions. Because the candidate solution violates the voltage magnitude lower bound constraint, the solution must be discarded and the optimization problem pronounced as infeasible.

A second IV-ACOPF scenario that reflects high loading conditions is now studied. This time, all currents have been increased by 23.3%. Now the IV-ACOPF optimization program reaches an optimum of $\mathcal{J} = \$757.56$. The associated decision variables are shown in Figure 6. In this scenario, Generator 3 has reached its real current capacity limit, while Generators 1 and 2 respectively are less than 1% and 2% away from their real current inject limits. Generator 1 continues to reach its imaginary current capacity limit. Again, as expected, the generator voltage magnitudes are all situated on their respective upper bounds. At these high loading conditions, Power Line 4 has reached its thermal capacity limit. Finally, because of the voltage magnitude relaxation, the voltage magnitudes for demand buses 3, 4, 5 and 6 are now all below the safe value of 0.9p.u by 0.299, 0.307, 1.11, and 1.84% respectively. Therefore, by Lemma 1, this candidate solution must be discarded and the optimization problem pronounced as infeasible. Figure 7 visualizes the candidate solution in a manner similar to that shown in Figure 3.

VI. DISCUSSION: THE IMPORTANCE OF MODELING DECISIONS

This paper has contributed a profit-maximizing security-constrained IV-ACOPF formulation as a convex optimization program which lends itself to a straightforward globally optimal solution via a Newton-Raphson algorithm. In so doing, it has demonstrated several modeling novelties which this section now discusses. The first decision was to switch away from $PQV\theta$ decision variables to IV decision variables. A $PQV\theta$ formulation inevitably introduces non-convex $|V_i||V_j|$ terms ($i \neq j$) in order to calculate the active power P and reactive power Q variables. Similarly, an $IVPQ$ formulation that mixes current, voltage, active power, and reactive power variables must inevitably introduce $S = V \star \mathcal{I}^*$ constraints which are also non-convex. Therefore, a whole-hearted flip into IV phasors is required to eliminate these non-convexities. Similarly, the choice of rectangular coordinates for these phasors rather than polar coordinates avoids the introduction of non-convex $\sin(\theta)$ and $\cos(\theta)$ terms. The result is a set of easily managed linear network flow constraints.

This IV-ACOPF also features a steady-state current injection model that includes generator terminals and their associated lead lines. This modeling decision has two primary advantages. First, the power flow analysis assumes complex power injections from generators; that when converted to IV variables imply that the generators are *current sources*. This modeling assumption is physically inconsistent with other electric machine models and power systems engineering models where generators are typically modeled as Thevenin-equivalent *voltage sources* [108], [113], [114]. The choice of voltage sources over current sources corrects the underlying *causality* [115], [116] of the system where the generator's current is *drawn* from the network rather than *imposed* by the generator. Second, the introduction of the generator lead lines in the current injection model means that the

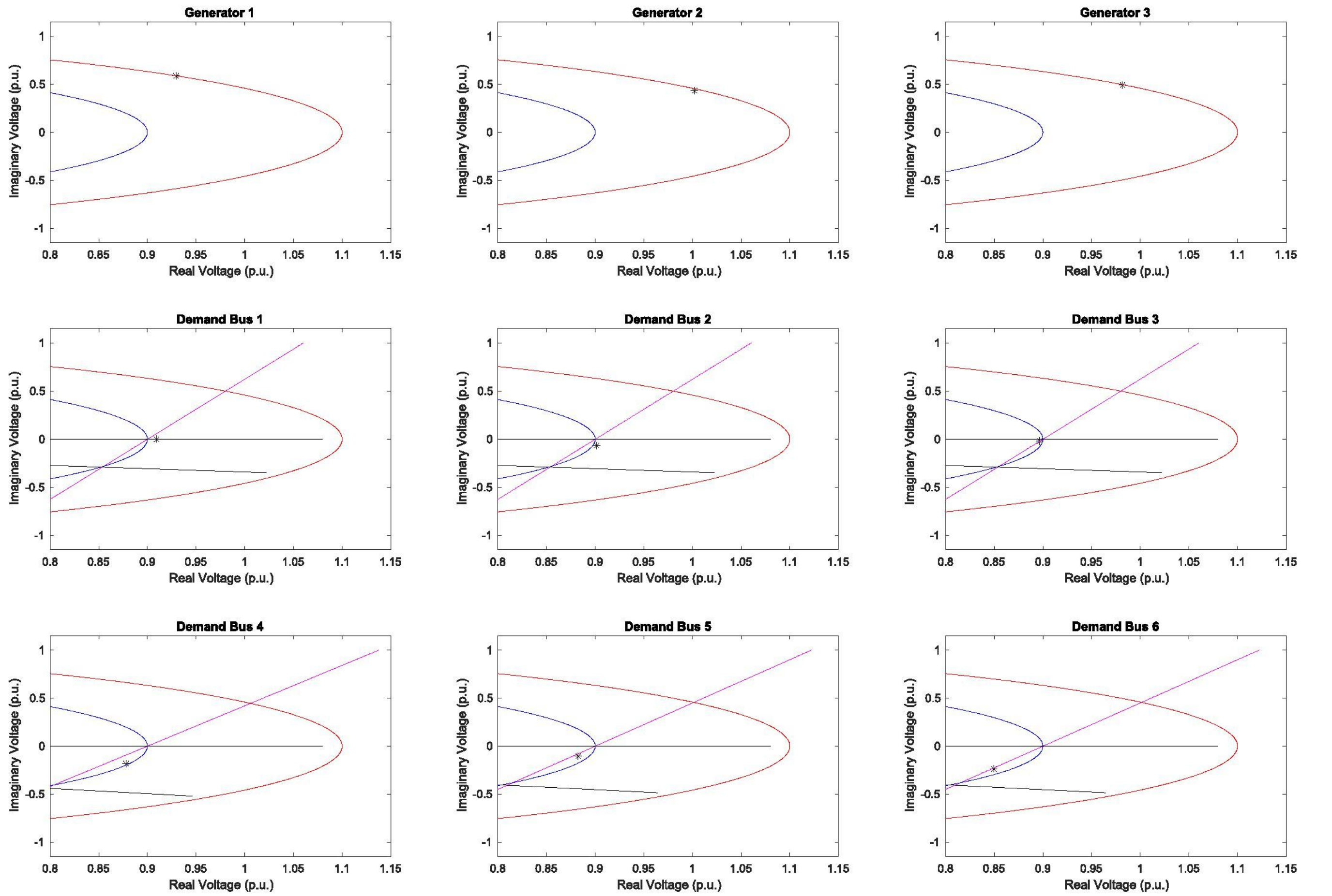

FIGURE 7. **The candidate nodal voltage solution $y^\dagger$ of the IV-ACOPF formulation under high loading conditions is indicated by *. Voltage upper bounds are shown in red. Voltage lower bounds are shown in blue. Voltage lower bound relaxations are shown in magenta. Power factor upper and lower bounds are shown in black. Each generator and demand bus is shown. Because the candidate solution violates the voltage magnitude lower bound constraint, the solution must be discarded, and the optimization problem pronounced as infeasible.**

supply-side of the objective function can now be expressed in terms of generator currents $\mathcal{I}_G$ alone and thus avoid the typical $S = V \star \mathcal{I}^*$ non-convexity when IV formulations must ultimately monetize the purchase and sale of active and reactive power. Said differently, the correction of the physical causality also corrects the mathematical non-convexity.

Along these lines, this IV-ACOPF formulation also takes special care in the design of the objective function. Typical ACOPF formulations that offer a one-sided cost minimization (as in Eq. 9) are just a mathematical short-hand for a two-sided profit maximization with inelastic demand as in Eq. 1. Nevertheless, the distinction in this work is critical because the explicit inclusion of the demand-side revenue terms (even if the demand is inflexible) is instrumental in the derivation of a convex objective function. Although this work continues with the traditional assumption of inelastic demand, this two-sided formulation indicates that one-sided market designs are perhaps outdated and that two-sided markets should become the norm in the context of the 21^{st} century sustainable energy transition. Follow-on works to this paper are likely to investigate elastic demand formulations. The objective function also monetizes both active and reactive power. Because traditional ACOPF formulations have been directed to transmission systems, they have often focused on active power generation and flow and neglected reactive power. In distribution systems, however, the flow of reactive power is often highly constrained. Therefore, this IV-ACOPF formulation provides the monetary incentive to alleviate these reactive power flow constraints. Furthermore, on the demand side, it charges differently for current delivered at one voltage versus another. In conclusion, the objective function gives balanced attention to the supply side, the demand side, active power and reactive power.

This IV-ACOPF formulation also pays special attention to the generator capacity constraints. In that regard, it is clear that the original 1962 paper by Carpentier approximates the capability curve of synchronous generators; which in turn is expressed as a constant voltage multiple of a synchronous generator's phasor diagram. In order to maintain consistency of the modeling, this work simply "undoes"

the multiplication of V_ϕ/X_S but retains the Carpentier's box constraints. This avoids several non-convexities from the synchronous generator's phasor diagram. It also facilitates a market design that is agnostic to device physics and treats all energy resources with the same level playing field; a highly desirable characteristic in the socio-economic design of an equitable electricity market.

The choice of exogeneous data in this IV-ACOPF formulation versus a traditional ACOPF is also of particular importance. The traditional ACOPF provides S_D as exogenous data. When switching to IV variables, this exogeneous data decision reveals two simultaneous dilemmas. First, and mathematically, $S_D = V_D \star \mathcal{I}_D^*$ immediately introduces a constraint of indefinite convexity. Second, and physically, electric power systems are based upon either voltage *or* current *causality*. Introducing exogeneous complex power consumption data S_D is a statement of ambiguous causality of power system physics. When receiving exogeneous data of complex power withdrawals, a power systems engineer should ask whether the underlying physics assumed voltage or current sinks with their associated imposition on causality. In the unlikely event that the load is a voltage sink, then the associated demand-bus voltage decision variable disappears. In contrast, if the load is a current sink (or a given impedance), then the demand-bus voltage remains as a decision variable as provided in this IV-ACOPF formulation. Although, existing ACOPF implementations have amassed considerable quantities of complex power demand data, the original source of this data normally collects the associated current phasor data as well; either from SCADA (Supervisory Control and Data Acquisition) systems or smart meters. Therefore, the benefits of changing exogeneous data from S_D to $\mathcal{I}_D$ greatly outweigh the relatively modest implementation effort. Similarly, existing forecasting software which normally predict S_D can be retooled with historical voltage phasor data V_D to produce $\mathcal{I}_D$. Alternatively, new forecasting software can predict $\mathcal{I}_D$ directly from historical current phasor data. The implementation steps avoid the use complex power data with indefinite convexity *and* ambiguous physical causality.

Finally, it is important to comment on the equivalence of this IV-ACOPF to the original ACOPF problem described in Sec. II.

Theorem 3: Given the optimal vector of demand-bus voltage phasors $V_D^\dagger$, the IV-ACOPF formulation defined by Equation 59-72 and 77 is a *generalization* of the ACOPF formulation defined by Equations 1-8 when P_D and $\mathcal{I}_D^*$ are chosen such that $S_D = V_D^\dagger \mathcal{I}_D^*$.

Proof: The equations of the IV-ACOPF are addressed in turn.

- By the discussion in Section III-C, the objective function in Eq. 59 is equivalent to Eq. 1 when $\alpha_{Ig} = \alpha_{Id} = \beta_{Ig} = \beta_{Id} = 0 \quad \forall g \in \mathcal{G}, d \in \mathcal{D}$.
- From the proof of Lemma 2, the network flow equations 60-63 are combined to yield Equation 88. Applying the definitions of Y_L, A_G and A_D to the bottom block-row of equations gives:

$$-\mathcal{I}_D = A_{DG}^T Y_{LG} A_{GG} V_G + A_{DG}^T Y_{LG} A_{DG} V_D + A_{DD}^T Y_{LD} A_{DD} V_D \quad (93)$$

Substituting in Ohm's Law on the lead lines from Eq. 15 and the definition of a bus admittance matrix $Y_D = Y_{LD}^T A_{DD} V_D$ gives:

$$-\mathcal{I}_D = A_{DG}^T I_{LG} + Y_{DD} V_D \quad (94)$$

This same result can be confirmed from the power analysis model by rewriting Equations 2 and 3 in complex matrix form:

$$A_{GD} S_G - S_D = diag(V_D) Y_D^* V_D^* \quad (95)$$

and then dividing all terms by $diag(V_D)$. Because S_D and $\mathcal{I}_D$ are exogeneous constants they must be related by the optimal vector of demand-bus voltage phasors $V_D^\dagger$. $S_D = V_D^\dagger \mathcal{I}_D^*$.
- By the discussion in Section III-D, the reference angle constraint in Eq. 64 is equivalent to Eq. 4.
- By the discussion in Section III-E, the generator capacity constraints in Equations 65 - 68 are equivalent to Equations 5 and 6.
- By the discussion in Section III-F, the thermal line flow constraint in Eq. 69 is equivalent to Eq. 7.
- By the discussion in Section III-G, the voltage magnitude constraints in Equations 73 and 77 are equivalent to Eq. 8.
- By the discussion in Section III-H, the exogeneous constant $S_D = P_D + jQ_D$ in the ACOPF is a specific condition of the power factor upper and lower bounds in Equations 71 and 72 where $\theta_{VD}^{max} = \theta_{VD}^{min}$ and $\theta_{VD} - \theta_{ID} = \tan^{-1}(Q_D/P_D)$. □

Note that Theorem 3 omits the generator terminal voltage upper bound because the generator terminals do not appear in the power flow analysis model of the ACOPF. Their re-inclusion serves to protect generators from over-voltages. Similarly, the theorem omits the voltage stability constraints in Equations 74 and 75 because they do not appear in the original ACOPF either. Their re-inclusion would protect the grid from voltage instabilities. Lastly, the voltage magnitude lower bound relaxation in Eq. 76 is superfluous in the presence of the more binding voltage magnitude lower bound in Eq. 77. In other words, and as a significant conclusion of this paper, when P_D and $\mathcal{I}_D^*$ are chosen such that $P_D = V_D^\dagger \mathcal{I}_D^*$ and $\alpha_{Ig} = \alpha_{Id} = \beta_{Ig} = \beta_{Id} = 0 \quad \forall g \in \mathcal{G}, d \in \mathcal{D}$, then the optimal point $x^* = [V_{RG}; V_{IG}; I_{RG}; I_{IG}; V_{RD}; V_{ID}]$ of the IV-ACOPF formulation defined by Equation 59-72 and 77 is equivalent to optimum point $\chi = [P_G; Q_G; |V_D|; \theta_D]$ from the ACOPF formulation defined by Equations 1-8.

Beyond these equivalence conditions, it is important to recognize that the more general conditions of the IV-ACOPF offer notable improvements. More specifically, relaxing the condition $P_D = V_D^\dagger \mathcal{I}_D^*$ means that the demand side is no longer a constant but rather a *function* of demand-bus

voltages. The original ACOPF 1.) ignores the demand side entirely and 2.) does not differentiate between the sale of electric power at one voltage versus another (assuming, perhaps incorrectly, that a customer is indifferent to voltage magnitude). Instead, the inclusion of these demand side terms as functions in the IV-ACOPF explicitly differentiates the sale of electric power at one voltage versus another. In a 21^{st} century sustainable energy transition characterized by the energy Internet of Things [36] and other demand side resources [117], it is likely that treating the sale of only active power integrated over time on a purely kWh basis irrespective of voltage level is no longer viable in the long-term. Furthermore, the use of exogeneous power demand data S_D was an immediate source of indefinite convexity *and* was an immediate source of ambiguous physical causality. The switch to exogeneous current demand $\mathcal{I}_D$ data alleviates both of these problems and a practical power systems engineer may ask why the (original) ACOPF should continue to be solved in light of these problems with S_D as the choice of exogeneous data. Setting aside these computational and practical benefits, in the end, the IV-ACOPF and ACOPF models both effectively secure the grid. While the IV-ACOPF formulation can be solved to global optimality in polynomial time, the original ACOPF, at present, can not.

VII. CONCLUSION

In conclusion, this paper has contributed a profit maximizing security-constrained current-voltage AC optimal power flow (IV-ACOPF) model and globally optimal algorithm. The main novelty of the work is its exclusive use of current and voltage phasors in rectangular coordinates to maintain the convexity of the optimization problem. The formulation also explicitly includes both the supply and demand sides to provide a profit maximizing rather than cost minimizing functionality. The now linear network flow constraints also facilitate the inclusion of power factor constraints (Eq. 47 and 48) and voltage stability constraints (Eq. 53 and 54) that are often neglected in typical optimal power flow formulations. This IV-ACOPF does feature a high quality "secant-line" relaxation on the otherwise non-convex voltage magnitude lower bound. This new IV-ACOPF reformulation facilitates a straightforward polynomial-time globally optimal solution via a Newton-Raphson algorithm. The numerical results confirm the globally optimal solution and return infeasible solutions when the loading conditions are excessively high. As elaborated in the discussion section, this paper opens the door to significant future work that enables the sustainable energy transition; including application to the operation of distribution systems and microgrids, two-sided markets with elastic demand, and coupling to other infrastructure sectors. It also is likely to have direct application to generation and transmission planning methods.

ACKNOWLEDGMENT

The authors would like to thank Prof. Kamal Youcef-Toumi, Prof. Massoud Amin, and Prof. Scott Moura for graciously reading and commenting on the work prior to its publication in IEEE Access., and their would also like to thank the anonymous IEEE Access reviewers for their suggestions on the clarity of the work.

NOMENCLATURE

DECISION VARIABLES

$\mid V_D \mid$	Magnitudes of Voltage Phasors for Demand Buses.
θ_{ID}	Phase Angle of Current Phasor for Demand Buses.
θ_{VD}	Phase Angle of Voltage Phasor for Demand Buses.
θ_{VD}^{max}	Upper Bound on Phase Angle of Voltage Phasor for Demand Buses.
θ_{VD}^{min}	Lower Bound on Phase Angle of Voltage Phasor for Demand Buses.
J	Profit Objective Functin.
MC_G	Marginal Revenue.
MR_D	Marginal Cost.
P_G	Active Power from Generators.
P_L	Active Power through Power Lines.
Q_G	Reactive Power from Generators.
Q_L	Reactive Power through Power Lines.
S_G	Complex Power from Generators.
S_L	Complex Power through Power Lines.
V_{DI}	Imaginary Part of Voltage Phasors for Demand Buses.
V_{DR}	Real Part of Voltage Phasors for Demand Buses.
V_D	Voltage Phasors for Demand Buses.
V_{GI}	Imaginary Part of Voltage Phasors for Generators.
V_{GR}	Real Part of Voltage Phasors for Generators.
V_G	Voltage Phasors for Generators.
$\mathcal{I}_{\mathcal{LDI}}$	Imaginary Part of Current Phasors for Demand Bus to Demand Bus Power Lines.
$\mathcal{I}_{\mathcal{LDR}}$	Real Part of Current Phasors for Demand Bus to Demand Bus Power Lines.
$\mathcal{I}_{\mathcal{LD}}$	Current Phasors for Demand Bus to Demand Bus Power Lines.
$\mathcal{I}_{\mathcal{LGI}}$	Imaginary Part of Current Phasors for Generator Lead Lines.
$\mathcal{I}_{\mathcal{LGR}}$	Real Part of Current Phasors for Generator Lead Lines.
$\mathcal{I}_{\mathcal{LG}}$	Current Phasors for Generator Lead Lines.
$\mathcal{I}_{\mathcal{LI}}$	Imaginary Part of Current Phasors for Power Lines.
$\mathcal{I}_{\mathcal{LR}}$	Real Part of Current Phasors for Power Lines.
$\mathcal{I}_{\mathcal{L}}$	Current Phasors for Power Lines.
$\mathcal{I}_{GI}$	Imaginary Part of Current Phasors for Generators.
$\mathcal{I}_{GR}$	Real Part of Current Phasors for Generators.
$\mathcal{I}_G$	Current Phasors for Generators.

OTHER SYMBOLS

$f()$	A Generic Function.
$g()$	A Generic Function.
$h()$	A Generic Function.
k	Iteration Counter.
$y^{\dagger}$	A Candidate Solution.

$y^\dagger$ An Optimal Solution.
$\mathcal{L}()$ A Lagrangian Function.
λ Lagrange Multipliers.
λ_e Eigenvalues.

PARAMETERS

α_{R_D} Quadratic Cost Coefficient for Active Power from Demand Buses.
α_{R_G} Quadratic Cost Coefficient for Active Power from Generators.
β_{R_D} Linear Cost Coefficient for Active Power from Demand Buses.
β_{R_G} Linear Cost Coefficient for Active Power from Generators.
γ_{R_D} Fixed Cost Coefficient for Active Power from Demand Buses.
γ_{R_G} Fixed Cost Coefficient for Active Power from Generators.
$\mid V_D \mid^{max}$ Upper Bound on Voltage Magnitude of Demand Buses.
$\mid V_D \mid^{min}$ Lower Bound on Voltage Magnitude of Demand Buses.
A_D Line-to-Bus Incidence Matrix.
A_{GD} Generator-to-Demand Bus Incidence Matrix.
A_G Line-to-Generator Incidence Matrix.
B Bus Susceptance Matrix.
B_L Generator & Bus Susceptance Matrix.
G Bus Conductance Matrix.
G_L Generator & Bus Conductance Matrix.
$N_{\mathcal{D}}$ Number of Demand Buses.
$N_{\mathcal{D}}$ Number of Power Lines.
$N_{\mathcal{G}}$ Number of Generators.
P_D Active Power from Demand Buses.
P_G^{max} Upper Bound on Active Power from Generators.
P_G^{min} Lower Bound on Active Power from Generators.
P_L^{max} Upper Bound on Active Power through Power Lines.
Q_D Reactive Power from Demand Buses.
Q_G^{max} Upper Bound on Reactive Power from Generators.
Q_G^{min} Lower Bound on Reactive Power from Generators.
S_D Complex Power from Demand Buses.
Y Bus Admittance Matrix.
Y_L Generator & Bus Admittance Matrix.
$\mathcal{I}_{DI}$ Imaginary Part of Current Phasors for Demand Buses.
$\mathcal{I}_{DR}$ Real Part of Current Phasors for Demand Buses.
$\mathcal{I}_D$ Current Phasors for Demand Buses.
$\mathcal{Y}_L$ Lead Line and Power Line Admittances.

SETS

$d \in \mathcal{D}$ Demand Buses.
$g \in \mathcal{G}$ Generators.
$l \in \mathcal{L}$ Power Lines.
$l \in \mathcal{L}_D$ Demand Bus to Demand Bus Power Lines.
$l \in \mathcal{L}_G$ Generator Lead Lines.
$\mathcal{R}_F$ Feasible Region.
$\mathcal{R}_{RF}$ Relaxed Feasible Region.
$\mathcal{R}_R$ Relaxed Region.

REFERENCES

[1] J. Carpentier, "Contribution to the economic dispatch problem," *Bull. Soc. Franc. Electr.*, vol. 3, no. 8, pp. 431–447, 1962.
[2] S. Frank and S. Rebennack, "A primer on optimal power flow: Theory, formulation, and practical examples," Colorado School of Mines, Golden, CO, USA, Tech. Rep. 2012-14, Oct. 2012, pp. 1–42.
[3] M. Cain, R. O'neill, and A. Castillo, "History of optimal power flow and formulations," Federal Energy Regulatory Commission, Washington, DC, USA, Tech. Rep. 1, 2012, pp. 1–36.
[4] A. Muzhikyan, S. O. Muhanji, G. D. Moynihan, D. J. Thompson, Z. M. Berzolla, and A. M. Farid, "The 2017 ISO new England system operational analysis and renewable energy integration study (SOARES)," *Energy Rep.*, vol. 5, pp. 747–792, Nov. 2019, doi: 10.1016/j.egyr.2019.06.005.
[5] *PJM Manual 11: Energy and Ancillary Services Market Operations*, PJM, Norristown, PA, USA, Oct. 2012.
[6] A. Garcia, L. Mili, and J. Momoh, "Modeling electricity markets: A brief introduction," in *Economic Market Design and Planning for Electric Power Systems*. Hoboken, NJ, USA: Wiley, 2009, pp. 21–44, doi: 10.1002/9780470529164.ch2.
[7] J. J. Shaw, "A direct method for security-constrained unit commitment," *IEEE Trans. Power Syst.*, vol. 10, no. 3, pp. 1329–1342, Aug. 1995.
[8] J. Wang, M. Shahidehpour, and Z. Li, "Security-constrained unit commitment with volatile wind power generation," *IEEE Trans. Power Syst.*, vol. 23, no. 3, pp. 1319–1327, Aug. 2008.
[9] J. D. Guy, "Security constrained unit commitment," *IEEE Trans. Power App. Syst.*, vol. PAS-90, no. 3, pp. 1385–1390, 1971.
[10] M. Vahedipour-Dahraei, H. R. Najafi, A. Anvari-Moghaddam, and J. M. Guerrero, "Security-constrained unit commitment in AC microgrids considering stochastic price-based demand response and renewable generation," *Int. Trans. Electr. Energy Syst.*, vol. 28, no. 9, p. e2596, Sep. 2018.
[11] S. L. Gbadamosi and N. I. Nwulu, "A comparative analysis of generation and transmission expansion planning models for power loss minimization," *Sustain. Energy, Grids Netw.*, vol. 26, Jun. 2021, Art. no. 100456.
[12] N. E. Koltsaklis and A. S. Dagoumas, "State-of-the-art generation expansion planning: A review," *Appl. Energy*, vol. 230, pp. 563–589, Nov. 2018.
[13] C. Li, A. J. Conejo, P. Liu, B. P. Omell, J. D. Siirola, and I. E. Grossmann, "Mixed-integer linear programming models and algorithms for generation and transmission expansion planning of power systems," *Eur. J. Oper. Res.*, vol. 297, no. 3, pp. 1071–1082, Mar. 2022.
[14] M. Moradi-Sepahvand and T. Amraee, "Integrated expansion planning of electric energy generation, transmission, and storage for handling high shares of wind and solar power generation," *Appl. Energy*, vol. 298, Sep. 2021, Art. no. 117137.
[15] D. K. Molzahn, C. Josz, I. A. Hiskens, and P. Panciatici, "A laplacian-based approach for finding near globally optimal solutions to OPF problems," *IEEE Trans. Power Syst.*, vol. 32, no. 1, pp. 305–315, Jan. 2017.
[16] P. P. C. Z. Silano Chen and P. A., "Optimal allocation of wind turbines in active distribution networks by using multi-period optimal power flow and genetic algorithms," in *Proc. Modeling Control Sustain. Power Syst.*, 2012, pp. 1–20.
[17] A. G. Bakirtzis, P. N. Biskas, C. E. Zoumas, and V. Petridis, "Optimal power flow by enhanced genetic algorithm," *IEEE Trans. Power Syst.*, vol. 17, no. 2, pp. 229–236, May 2002.
[18] S. R. Paranjothi and K. Anburaja, "Optimal power flow using refined genetic algorithm," *Electr. Power Compon. Syst.*, vol. 30, no. 10, pp. 1055–1063, Oct. 2002.
[19] M. S. Osman, M. A. Abo-Sinna, and A. A. Mousa, "A solution to the optimal power flow using genetic algorithm," *Appl. Math. Comput.*, vol. 155, no. 2, pp. 391–405, Aug. 2004.
[20] D. Devaraj and B. Yegnanarayana, "Genetic-algorithm-based optimal power flow for security enhancement," *IEE Proc.-Gener., Transmiss. Distrib.*, vol. 152, no. 6, pp. 899–905, Nov. 2005.
[21] U. Leeton, D. Uthitsunthorn, U. Kwannetr, N. Sinsuphun, and T. Kulworawanichpong, "Power loss minimization using optimal power flow based on particle swarm optimization," in *Proc. Int. Conf. onElectr. Eng./Electron. Comput. Telecommun. Inf. Technol. (ECTI-CON)*, 2010, pp. 440–444.
[22] E. Sortomme and M. A. El-Sharkawi, "Optimal power flow for a system of microgrids with controllable loads and battery storage," in *Proc. IEEE/PES Power Syst. Conf. Expo.*, Mar. 2009, pp. 1–5.

[23] M. A. Abido, "Optimal power flow using particle swarm optimization," *Int. J. Elect. Power Energy Syst.*, vol. 24, no. 7, pp. 563–571, 2002.
[24] S. He, J. Y. Wen, E. Prempain, Q. H. Wu, J. Fitch, and S. Mann, "An improved particle swarm optimization for optimal power flow," in *Proc. Int. Conf. Power Syst. Technol. PowerConf.*, 2013, pp. 1–40.
[25] J. Hazra and A. K. Sinha, "A multi-objective optimal power flow using particle swarm optimization," *Eur. Trans. Electr. Power*, vol. 21, no. 1, pp. 1028–1045, Jan. 2011.
[26] C.-R. Wang, H.-J. Yuan, Z.-Q. Huang, J.-W. Zhang, and C.-J. Sun, "A modified particle swarm optimization algorithm and its application in optimal power flow problem," in *Proc. Int. Conf. Mach. Learn. Cybern.*, vol. 5, Aug. 2005, pp. 2885–2889.
[27] R.-H. Liang, S.-R. Tsai, Y.-T. Chen, and W.-T. Tseng, "Optimal power flow by a fuzzy based hybrid particle swarm optimization approach," *Electr. Power Syst. Res.*, vol. 81, no. 7, pp. 1466–1474, 2011.
[28] C. A. Roa-Sepulveda and B. J. Pavez-Lazo, "A solution to the optimal power flow using simulated annealing," *Int. J. Electr. Power Energy Syst.*, vol. 25, no. 1, pp. 47–57, 2003.
[29] T. Sousa, J. Soares, Z. Vale, H. Morais, and P. Faria, "Simulated annealing metaheuristic to solve the optimal power flow," in *Proc. IEEE Power Energy Soc. Gen. meeting*, Apr. 2011, pp. 1–8.
[30] T. Niknam, M. R. Narimani, and M. Jabbari, "Dynamic optimal power flow using hybrid particle swarm optimization and simulated annealing," *Int. Trans. Electr. Energy Syst.*, vol. 23, no. 7, pp. 975–1001, Oct. 2013.
[31] V. J. Gutierrez-Martinez, C. A. Canizares, C. R. Fuerte-Esquivel, A. Pizano-Martinez, and X. Gu, "Neural-network security-boundary constrained optimal power flow," *IEEE Trans. Power Syst.*, vol. 26, no. 1, pp. 63–72, Feb. 2011.
[32] P. Siano, C. Cecati, H. Yu, and J. Kolbusz, "Real time operation of smart grids via FCN networks and optimal power flow," *IEEE Trans. Ind. Informat.*, vol. 8, no. 4, pp. 944–952, Nov. 2012.
[33] X. Pan, T. Zhao, and M. Chen, "DeepOPF: Deep neural network for DC optimal power flow," in *Proc. IEEE Int. Conf. Commun., Control, Comput. Technol. Smart Grids*, Oct. 2019, pp. 1–6.
[34] X. Pan, M. Chen, T. Zhao, and S. H. Low, "DeepOPF: A feasibility-optimized deep neural network approach for AC optimal power flow problems," 2020, *arXiv:2007.01002*.
[35] S. Frank, I. Steponavice, and S. Rebennack, "Optimal power flow: A bibliographic survey II," *Energy Syst.*, vol. 3, no. 3, pp. 259–289, Sep. 2012.
[36] S. O. Muhanji, A. E. Flint, and A. M. Farid, *EIoT: The Development Energy Internet Things Energy Infrastructure*. Berlin, Germany: Springer, 2019, doi: 10.1007/978-3-030-10427-6.
[37] C. Cecati, C. Citro, A. Piccolo, and P. Siano, "Smart grid operation with distributed generation and demand side management," in *Modeling and Control of Sustainable Power Systems*. Berlin, Germany: Springer, 2012, pp. 27–81.
[38] L. Wang, *Modeling and Control of Sustainable Power Systems, Wang and Lingfeng*, L. Wang, Ed. Berlin, Germany: Springer, 2012.
[39] G. Ferruzzi, G. Graditi, F. Rossi, and A. Russo, "Optimal operation of a residential microgrid: The role of demand side management," *Intell. Ind. Syst.*, vol. 1, no. 1, pp. 61–82, Jun. 2015.
[40] D. Gayme and U. Topcu, "Optimal power flow with large-scale storage integration," *IEEE Trans. Power Syst.*, vol. 28, no. 2, pp. 709–717, May 2013.
[41] F. A. Rahimi and A. Ipakchi, "Transactive energy techniques: Closing the gap between wholesale and retail markets," *Electr. J.*, vol. 25, no. 8, pp. 29–35, 2012.
[42] *Pacific Northwest Gridwise Testbed Demonstration Projects: Part 2. Grid-Friendly Appliances Project*, Pacific Northwest Nat. Lab., Richland, WA, USA, 2007.
[43] *Pacific Northwest Gridwise Testbed Demonstration Projects Part 1. Olympic Peninsula Project*, Pacific Northwest Nat. Lab., Richland, WA, USA, 2007.
[44] D. Hammerstrom, R. Ambrosio, J. Brous, T. Carlon, D. Ghassin, J. DeSteese, R. Guttromson, G. Horst, O. Järregren, and R. Kajfasz, "Pacific northwest gridwise TM testbed demonstration projects, volume I: The Olympic peninsula project," Pacific Northwest Nat. Lab., Richland, WA, USA, Tech. Rep. PNNL-17167, 2007.
[45] S. E. Widergren, K. Subbarao, J. C. Fuller, D. P. Chassin, A. Somani, M. C. Marinovici, and J. L. Hammerstrom, "AEP Ohio gridSMART demonstration project real-time pricing demonstration analysis," Pacific Northwest Nat. Lab., Richland, WA, USA, Tech. Rep. 45, 2014.
[46] W.-C. Lin and H. E. Garcia, "Inclusion of game-theoretic formulations for resilient condition assessment monitoring," in *Proc. 6th Int. Symp. Resilient Control Syst. (ISRCS)*, Aug. 2013, pp. 96–103, doi: 10.1109/ISRCS.2013.6623758.
[47] V. Hosseinnezhad, M. Rafiee, M. Ahmadian, and P. Siano, "Optimal day-ahead operational planning of microgrids," *Energy Convers. Manage.*, vol. 126, pp. 142–157, Oct. 2016. [Online]. Available: http://www.sciencedirect.com/science/article/pii/S0196890416306549
[48] E. Dall'Anese, H. Zhu, and G. B. Giannakis, "Distributed optimal power flow for smart microgrids," *IEEE Trans. Smart Grid*, vol. 4, no. 3, pp. 1464–1475, Sep. 2013.
[49] Y. Levron, J. M. Guerrero, and Y. Beck, "Optimal power flow in microgrids with energy storage," *IEEE Trans. Power Syst.*, vol. 28, no. 3, pp. 3226–3234, Aug. 2013.
[50] H. Gao, J. Liu, L. Wang, and Z. Wei, "Decentralized energy management for networked microgrids in future distribution systems," *IEEE Trans. Power Syst.*, vol. 33, no. 4, pp. 3599–3610, Jul. 2018.
[51] *Investor-Owned Utilities Served 72% of U.S. Electricity Customers in 2017*, U.S. Energy Inf. Admin., Washington, DC, USA, Aug. 2019. [Online]. Available: https://www.eia.gov/todayinenergy/detail.php?id=40913
[52] D. Molzahn, F. Dörfler, and H. Sandberg, "A survey of distributed optimization and control algorithms for electric power systems," *IEEE Trans. Smart Grid*, vol. 8, no. 6, pp. 2941–2962, Nov. 2017.
[53] S. O. Muhanji, A. Muzhikyan, and A. M. Farid, "Distributed control for distributed energy resources: Long-term challenges and lessons learned," *IEEE Access*, vol. 6, pp. 32737–32753, 2018, doi: 10.1109/ACCESS.2018.2843720.
[54] S. O. Muhanji, A. Muzhikyan, and A. M. Farid, "Long-term challenges for future electricity markets with distributed energy resources," in *Smart Grid Control: An Overview Res. Opportunities*, J. Stoustrup, A. M. Annaswamy, A. Chakrabortty, and Z. Qu, Eds. Berlin, Germany: Springer, 2017, pp. 59–81, doi: 10.1007/978-3-319-98310-3.
[55] A. Santhosh, A. M. Farid, and K. Youcef-Toumi, "Real-time economic dispatch for the supply side of the energy-water nexus," *Appl. Energy*, vol. 122, pp. 42–52, Jun. 2014, doi: 10.1016/j.apenergy.2014.01.062.
[56] A. Santhosh, A. M. Farid, and K. Youcef-Toumi, "The impact of storage facility capacity and ramping capabilities on the supply side of the energy-water nexus," *Energy*, vol. 66, no. 1, pp. 1–10, 2014, doi: 10.1016/j.energy.2014.01.031.
[57] W. N. Lubega and A. M. Farid, "Quantitative engineering systems modeling and analysis of the energy–water nexus," *Appl. Energy*, vol. 135, pp. 142–157, Dec. 2014, doi: 10.1016/j.apenergy.2014.07.101.
[58] W. Hickman, A. Muzhikyan, and A. M. Farid, "The synergistic role of renewable energy integration into the unit commitment of the energy water nexus," *Renew. Energy*, vol. 108, pp. 220–229, Aug. 2017, doi: 10.1016/j.renene.2017.02.063.
[59] A. M. Farid, "A hybrid dynamic system model for multi-modal transportation electrification," *IEEE Trans. Control Syst. Technol.*, vol. 25, no. 3, pp. 940–951, May 2016, doi: 10.1109/TCST.2016.2579602.
[60] W. C. Schoonenberg and A. M. Farid, "A dynamic model for the energy management of microgrid-enabled production systems," *J. Cleaner Prod.*, vol. 1, no. 1, pp. 1–10, 2017, doi: 10.1016/j.jclepro.2017.06.119.
[61] M. Cvetkovic and A. Annaswamy, "Coupled ISO-NE real-time energy and regulation markets for reliability with natural gas," in *Proc. IEEE Power Energy Soc. Gen. Meeting*, Jul. 2015, pp. 1–5.
[62] C. M. Correa-Posada and P. Sanchez-Martin, "Security-constrained optimal power and natural-gas flow," *IEEE Trans. Power Syst.*, vol. 29, no. 4, pp. 1780–1787, Jul. 2014.
[63] C. Liu, M. Shahidehpour, Y. Fu, and Z. Li, "Security-constrained unit commitment with natural gas transmission constraints," *IEEE Trans. Power Syst.*, vol. 24, no. 3, pp. 1523–1536, Aug. 2009.
[64] T. Li, M. Eremia, and M. Shahidehpour, "Interdependency of natural gas network and power system security," *IEEE Trans. Power Syst.*, vol. 23, no. 4, pp. 1817–1824, Nov. 2008.
[65] E. M. Wanjiru, S. M. Sichilalu, and X. Xia, "Model predictive control of heat pump water heater-instantaneous shower powered with integrated renewable-grid energy systems," *Appl. Energy*, vol. 204, pp. 1333–1346, Oct. 2017.
[66] P. Mancarella, "MES (multi-energy systems): An overview of concepts and evaluation models," *Energy*, vol. 65, pp. 1–17, Feb. 2014.
[67] Z. Li, W. Wu, M. Shahidehpour, J. Wang, and B. Zhang, "Combined heat and power dispatch considering pipeline energy storage of district heating network," *IEEE Trans. Sustain. Energy*, vol. 7, no. 1, pp. 12–22, Jan. 2016.
[68] H. Lund, S. Werner, R. Wiltshire, S. Svendsen, J. E. Thorsen, F. Hvelplund, and B. V. Mathiesen, "4th generation district heating (4GDH): Integrating smart thermal grids into future sustainable energy systems," *Energy*, vol. 68, pp. 1–11, Apr. 2014.

[69] *Nerc White Paper on Ferc Nopr [Docket rm16-1-000] Proposal to Revise Standard Generator Interconnection Agreements*, NERC, Atlanta, GA, USA, 2016.
[70] A. Ellis, R. Nelson, and E. Von Engeln, "Review of existing reactive power requirements for variable generation," in *Proc. IEEE Power Energy Soc. Gen. Meeting*, Apr. 2012, pp. 1–7.
[71] M. Huneault and F. D. Galiana, "A survey of the optimal power flow literature," *IEEE Trans. Power Syst.*, vol. 6, no. 2, pp. 762–770, May 1991.
[72] J. A. Momoh, M. E. El-Hawary, and R. Adapa, "A review of selected optimal power flow literature to 1993. II. Newton, linear programming and interior point methods," *IEEE Trans. Power Syst.*, vol. 14, no. 1, pp. 96–104, Feb. 1999.
[73] J. A. Momoh, R. Adapa, and M. E. El-Hawary, "A review of selected optimal power flow literature to 1993. Iw. Nonlinear and quadratic programming approaches," *IEEE Trans. Power Syst.*, vol. 14, no. 1, pp. 96–104, Feb. 1999.
[74] S. Frank, I. Steponavice, and S. Rebennack, "Optimal power flow: A bibliographic survey I," *Energy Syst.*, vol. 3, no. 3, pp. 221–258, Sep. 2012.
[75] R. P. O'Neill, A. Castillo, and M. B. Cain, "The IV formulation and linear approximations of the AC optimal power flow problem," Federal Energy Regulatory Commission, Washington, DC, USA, Tech. Rep., Dec. 2012.
[76] A. Castillo and R. P. O'Neill, "Survey of approaches to solving the ACOPF," Federal Energy Regulatory Commission, Washington, DC, USA, Tech. Rep., Mar. 2013.
[77] K. Pandya and S. Joshi, "A survey of optimal power flow methods," *J. Theor. Appl. Inf. Technol.*, vol. 4, pp. 450–458, Jan. 2008.
[78] E. Mohagheghi, M. Alramlawi, A. Gabash, and P. Li, "A survey of real-time optimal power flow," *Energies*, vol. 11, no. 11, p. 3142, 2018.
[79] D. Molzahn and I. Hiskens, *A Survey of Relaxations and Approximations of the Power Flow Equations*. Now, 2019, doi: 10.1561/3100000012.
[80] P. Schavemaker and L. Van der Sluis, *Electrical Power System Essentials*. Chichester, U.K.: Wiley, 2008. [Online]. Available: http://www.loc.gov/catdir/enhancements/fy0810/2008007359-d.html
[81] K. Dvijotham and D. K. Molzahn, "Error bounds on the DC power flow approximation: A convex relaxation approach," in *Proc. IEEE 55th Conf. Decis. Control (CDC)*, Dec. 2016, pp. 2411–2418.
[82] R. A. Jabr, "Radial distribution load flow using conic programming," *IEEE Trans. Power Syst.*, vol. 21, no. 3, pp. 1458–1459, Aug. 2006.
[83] R. A. Jabr, "Optimal power flow using an extended conic quadratic formulation," *IEEE Trans. Power Syst.*, vol. 23, no. 3, pp. 1000–1008, Aug. 2008, doi: 10.1109/TPWRS.2008.926439.
[84] X. Bai, H. Wei, K. Fujisawa, and Y. Wang, "Semidefinite programming for optimal power flow problems," *Elect. Power Energy Syst.*, vol. 30, no. 6, pp. 383–392, Dec. 2008.
[85] D. K. Molzahn, B. C. Lesieutre, and C. L. DeMarco, "Investigation of non-zero duality gap solutions to a semidefinite relaxation of the optimal power flow problem," in *Proc. 47th Hawaii Int. Conf. Syst. Sci.*, Jan. 2014, pp. 2325–2334.
[86] J. Lavaei and S. H. Low, "Zero duality gap in optimal power flow problem," *IEEE Trans. Power Syst.*, vol. 27, no. 1, pp. 92–107, Feb. 2012.
[87] C. Coffrin, H. L. Hijazi, and P. Van Hentenryck, "The QC relaxation: A theoretical and computational study on optimal power flow," *IEEE Trans. Power Syst.*, vol. 31, no. 4, pp. 3008–3018, Jul. 2016.
[88] S. Sojoudi and J. Lavaei, "Network topologies guaranteeing zero duality gap for optimal power flow problem," Dept. Ind. Eng. Oper. Res., Univ. California Berkeley, Berkeley, CA, USA, Tech. Rep., 2011.
[89] R. Madani, S. Sojoudi, and J. Lavaei, "Convex relaxation for optimal power flow problem: Mesh networks," *IEEE Trans. Power Syst.*, vol. 30, no. 1, pp. 199–211, May 2015.
[90] S. H. Low, "Convex relaxation of optimal power flow—Part I: Formulations and equivalence," *IEEE Trans. Control Netw. Syst.*, vol. 1, no. 2, pp. 15–27, Mar. 2014.
[91] R. P. O'neill, A. Castillo, and M. B. Cain, "The computational testing of AC optimal power flow using the current voltage formulations," Federal Energy Regulatory Commission, Washington, DC, USA, Tech. Rep., Dec. 2012.
[92] J. F. Franco, M. J. Rider, and R. Romero, "A mixed-integer linear programming model for the electric vehicle charging coordination problem in unbalanced electrical distribution systems," *IEEE Trans. Smart Grid*, vol. 6, no. 5, pp. 2200–2210, Sep. 2015.
[93] Z. Jiang, F. Li, W. Qiao, H. Sun, H. Wan, J. Wang, Y. Xia, Z. Xu, and P. Zhang, "A vision of smart transmission grids," in *Proc. IEEE Power Energy Soc. Gen. Meeting*, Jul. 2009, pp. 1–10, doi: 10.1109/PES.2009.5275431.
[94] H. Saadat, *Power System Analysis*, vol. 2. New York, NY, USA: McGraw-Hill, 1999.
[95] A. Gómez-Expósito, A. J. Conejo, and C. Ca nizares, *Electric Energy Systems: Analysis Operation*. Boca Raton, FL, USA: CRC Press, 2018.
[96] B. Cui and X. A. Sun, "A new voltage stability-constrained optimal power-flow model: Sufficient condition, SOCP representation, and relaxation," *IEEE Trans. Power Syst.*, vol. 33, no. 5, pp. 5092–5102, Sep. 2018.
[97] S. Kim, T. Song, M. Jeong, B. Lee, Y. Moon, J. Namkung, and G. Jang, "Development of voltage stability constrained optimal power flow (VSCOPF)," in *Proc. Power Eng. Soc. Summer Meeting. Conf. Process.*, vol. 3, Oct. 2001, pp. 1664–1669.
[98] Q. Wang and X. Sun, "The international journal of production research in the past, the present and the future: A bibliometric analysis," *Int. J. Prod. Res.*, vol. 57, nos. 15–16, pp. 4676–4691, Aug. 2019.
[99] R. J. Avalos, C. A. Canizares, and M. F. Anjos, "A practical voltage-stability-constrained optimal power flow," in *Proc. IEEE Power Energy Soc. Gen. Meeting-Convers. Del. Electr. Energy*, Feb. 2008, pp. 1–6.
[100] S. Boyd and L. Vandenberghe, *Numerical Optimization*. Cambridge, U.K.: Cambridge Univ. Press, 2004.
[101] J. Nocedal and S. J. Wright, *Numerical Optimization*. Berlin, Germany: Springer, 2006.
[102] L. K. Kirchmayer, *Economic Operation Power System*. New York, NY, USA: Wiley, 1958.
[103] G. Golub and C. Van Loan, *Matrix Computations*. Baltimore, MD, USA: Johns Hopkins University Press, 1996.
[104] D. R. Biggar and M. R. Hesamzadeh, *The Economics of Electricity Markets*. Hoboken, NJ, USA: Wiley, 2014.
[105] J. M. Morales, A. J. Conejo, H. Madsen, P. Pinson, and M. Zugno, *Integrating Renewables in Electricity Markets: Operational Problems*, vol. 205. Berlin, Germany: Springer, 2013.
[106] J. Momoh and L. Mili, *Economic Market Design and Planning for Electric Power Systems*, vol. 52. Hoboken, NJ, USA: Wiley, 2009.
[107] M. Shahidehpour and Z. Li, *Elecitricity Market Economics*. New York, NY, USA: Wiley, 2005.
[108] S. Chapman, *Electric Machinery Fundamentals*. New York, NY, USA: McGraw-Hill, 2005.
[109] A. J. Wood, B. F. Wollenberg, and G. B. Sheblé, *Power Generation, Operation, and Control*. Hoboken, NJ, USA: Wiley, 2013.
[110] F. A. Potra and S. J. Wright, "Interior-point methods," *J. Comput. Appl. Math.*, vol. 124, nos. 1–2, pp. 281–302, Jan. 2000.
[111] Anonymous. (2021). *Newton's Method*. [Online]. Available: https://en.citizendium.org/wiki/Newton's_method
[112] T. J. Ypma, "Historical development of the Newton–Raphson method," *SIAM Rev.*, vol. 37, no. 4, pp. 531–551, 1995.
[113] A. Gomez-Exposito, A. J. Conejo, and C. Canizares, *Electric Energy Systems: Analysis and Operation*. Boca Raton, FL, USA: CRC Press, 2008.
[114] J. L. Kirtley, *Electric Power Principles: Sources, Conversion, Distribution Use*. Hoboken, NJ, USA: Wiley, 2011.
[115] D. Karnopp, D. L. Margolis, and R. C. Rosenberg, *System Dynamics: A Unified Approach*, 2nd ed. New York, NY, USA: Wiley, 1990. [Online]. Available: http://www.loc.gov/catdir/enhancements/fy0650/90012110-t.html
[116] F. T. Brown, *Engineering System Dynamics*, 2nd ed. Boca Raton, FL: CRC Press, 2007.
[117] P. Palensky and D. Dietrich, "Demand side management: Demand response, intelligent energy systems, and smart loads," *IEEE Trans. Ind. Informat.*, vol. 7, no. 3, pp. 381–388, Aug. 2011.

AMRO M. FARID (Senior Member, IEEE) received the B.Sc. degree, in 2000, the M.Sc. degree in mechanical engineering from MIT, in 2002, and the Ph.D. degree in engineering from the University of Cambridge, U.K. He is currently a Visiting Associate Professor of Mechanical Engineering at MIT and an Associate Professor in Engineering at the Thayer School of Engineering, Dartmouth College. He leads the Laboratory for Intelligent Integrated Networks of Engineering Systems (LIINES) and has authored over 150 peer-reviewed publications in smart power grids, energy-water nexus, electrified transportation systems, industrial energy management, and interdependent smart city infrastructures. He holds leadership positions in the IEEE Smart Cities Program, Control Systems Society (CSS), the Power & Energy Society (PES), and the Systems, Man & Cybernetics Society (SMCS).